JOURNAL OF VIROLOGY, Apr. 2010, p. 3421–3430 Vol. 84, No. 7
0022-538X/10/$12.00 doi:10.1128/JVI.02416-09

Expression of Varicella-Zoster Virus Immediate-Early Regulatory Protein IE63 in Neurons of Latently Infected Human Sensory Ganglia▽

Leigh Zerboni,[1]* Raymond A. Sobel,[2] Vasavi Ramachandran,[1] Jaya Rajamani,[1] William Ruyechan,[3] Allison Abendroth,[4] and Ann Arvin[1]

Departments of Pediatrics and Microbiology and Immunology, Stanford University School of Medicine, Stanford, California 94305[1]; Department of Pathology, Stanford University School of Medicine, Stanford, California 94305[2]; Department of Microbiology and Immunology, University at Buffalo, State University of New York, Buffalo, New York 14201[3]; and Immunology and Infectious Diseases, University of Sydney, Sydney, Australia[4]

Received 16 November 2009/Accepted 15 January 2010

Varicella-zoster virus (VZV) causes varicella and establishes latency in sensory nerve ganglia, but the characteristics of VZV latency are not well defined. Immunohistochemical detection of the VZV immediate-early 63 (IE63) protein in ganglion neurons has been described, but there are significant discrepancies in estimates of the frequency of IE63-positive neurons, varying from a rare event to abundant expression. We examined IE63 expression in cadaver ganglia using a high-potency rabbit anti-IE63 antibody and corresponding preimmune serum. Using standard immunohistochemical techniques, we evaluated 10 ganglia that contained VZV DNA from seven individuals. These experiments showed that neuronal pigments were a confounding variable; however, by examining sections coded to prevent investigator bias and applying statistical analysis, we determined that IE63 protein, if present, is in a very small proportion of neurons (<2.8%). To refine estimates of IE63 protein abundance, we modified our protocol by incorporating a biological stain to exclude the pigment signal and evaluated 27 ganglia from 18 individuals. We identified IE63 protein in neurons within only one ganglion, in which VZV glycoprotein E and an immune cell infiltrate were also demonstrated. Antigen preservation was shown by detection of neuronal synaptophysin. These data provide evidence that the expression of IE63 protein, which has been referred to as a latency-associated protein, is rare. Refining estimates of VZV protein expression in neurons is important for developing a hypothesis about the mechanisms by which VZV latency may be maintained.

Varicella-zoster virus (VZV), the human alphaherpesvirus that causes varicella during primary infection, establishes a lifelong latency in neurons of the sensory ganglia along the cerebrospinal axis (7). Sensory ganglia are composed of heterogeneous populations of neurons surrounded by satellite cells and other nonneuronal cells; axons extend from these neurons to innervate the skin and mucous membranes (50). Herpes zoster (shingles) results from reactivation of latent virus within ganglion cells and transfer of newly synthesized infectious particles to the skin via axonal transport (7).

The number and type of neural cells that harbor latent virus are fundamental to the question of VZV latency. Studies to address this question have used methods to detect viral DNA, RNA, and proteins in cadaver ganglia. Although RNA is especially vulnerable to RNA-degrading enzymes during the postmortem interval between death and fixation of histological specimens at autopsy, DNA and proteins are reasonably stable (16). Nevertheless, reports using either VZV DNA or protein detection to assess the numbers of cells that contain VZV in human cadaver ganglia have yielded estimates that are extremely variable. By *in situ* hybridization and PCR methods, VZV DNA has been reported in as few as 1.5% of neurons exclusively (none in satellite cells) to as many as 30% of ganglion cells (neurons as well as satellite cells) (24, 26). Most recently, Wang et al. used a laser-capture microdissection/PCR method to provide more precise information at the single-cell level by examining 1,722 neurons in trigeminal ganglia (TGG) from seven individuals (49). These experiments identified VZV DNA in 4.1% of neurons (range, 1.0 to 6.9%) (49).

The first report of VZV protein expression in latently infected human ganglia was by Mahalingam and colleagues (29), who evaluated the immediate early 63 (IE63) protein encoded by VZV open reading frame 63 (ORF63). IE63 protein is a tegument/regulatory protein that contributes to VZV gene regulation by interaction with the viral transactivator, IE62, RNA polymerase II, and the cellular EF-1α promoter in the infected-cell nucleus (28, 53). In their study, IE63 was detected in very rare neurons in five ganglia from two adults but was not found in multiple tissue sections of 16 ganglia from seven other adults (29). In contrast, in the second of the four reports that have assessed the frequency of IE63-positive cells in cadaver ganglia, Lungu et al. (27) found IE63 protein in all of three cadaver dorsal root ganglia (DRG), with 3 to 9% of 200 neurons being positive in each tissue section; IE63 was localized to the cytoplasm (27). Kennedy et al. identified cells expressing IE63 protein in trigeminal ganglia from 5 of 20 subjects (19); as described by Mahalingam et al., it was necessary to examine a large number of sections from each patient to identify an IE63-positive cell (19). However, Grinfeld et al. subsequently reported IE63 expression in all ganglia from 10 subjects (one ganglion studied per subject); they estimated that 5 to 10% of neurons were positive although they noted that the patchy and

* Corresponding author. Mailing address: Stanford University School of Medicine, S-356, 300 Pasteur Dr., Stanford, CA 94305. Phone: (650) 723-6353. Fax: (650) 725-8040. E-mail: zerboni@stanford.edu.

▽ Published ahead of print on 27 January 2010.

focal distribution of labeling did not allow accurate quantitation (14). While not described as such in any of these reports, this protein has been referred to as the VZV latency-associated protein.

As might be expected given RNA instability postmortem, detection of mRNA transcripts for IE63 in cadaver ganglia has also been inconsistent. In one study, ORF63 was determined by reverse transcription-PCR (RT-PCR) to be the most abundantly transcribed VZV gene in latently infected neurons; however, two global searches for latently transcribed genes did not detect IE63 transcripts (8) (9). Full-length IE63 mRNA has not been demonstrated in latently infected human cadaver ganglia.

Our study was undertaken because, despite careful effort, there is substantial discordance among the four reports estimating the number of neurons that express IE63 protein in latently infected ganglia. That these range from a rare event found in two to four neurons per section in a fraction of ganglia examined to 5 to 10% of neurons per section in all ganglia examined suggested the need for further investigation. Therefore, we evaluated a large number of sections prepared from 27 ganglia from 18 individuals for IE63 expression. In our experiments, samples were coded to avoid bias and tested with a high-potency rabbit anti-IE63 antibody and the corresponding preimmune rabbit serum and with an alternative staining protocol that eliminates the signal associated with neuronal cell pigments. Our analysis is consistent with the reports by Mahalingam et al. and Kennedy et al. showing that IE63 protein expression occurs in latently infected neurons, but this expression is rare and, in some cases, may indicate an early stage of VZV reactivation in the absence of skin lesions typical of herpes zoster (29).

MATERIALS AND METHODS

Tissue specimens. Twenty-seven ganglia from 18 patients were examined; 6 were TGG and 21 were DRG. Twenty tissue blocks or sections from 14 patients were obtained from the VZV Research Foundation Tissue Bank (kindly provided by A. Gershon, Columbia University, New York, NY) or from the University of Sydney (Sydney, Australia). Seven cadaver ganglia were collected at autopsy from four patients by the Stanford University Medical Center Department of Pathology under an exempt protocol reviewed by the Stanford University Institutional Review Board. Ganglia were collected within 48 h of patient demise and immediately fixed in neutral-buffered formalin or 4% paraformaldehyde. All patients were without clinical evidence of herpes zoster when they died.

VZV-infected and uninfected human DRG xenografts, which contain organotypic features of adult ganglia, were used as positive and negative controls for immunohistochemical staining experiments; they were constructed by xenotransplantation and subsequent VZV infection of a human fetal ganglion in severe compromised immunodeficient (SCID) mouse, as previously described (52). DRG xenografts were collected at necropsy, fixed and preserved in paraffin blocks, and sectioned in a manner similar to that for cadaver ganglia. VZV-infected DRG xenografts were examined at 14 days postinoculation (acute phase, positive control); uninfected DRG xenografts were used as a negative control. VZV-infected DRG xenografts were also examined at 56 days postinfection, at which point the virus persists in a nonreplicating state, and gene transcription is restricted such that mRNAs corresponding to IE63 but not glycoprotein B are detected by real-time quantitative PCR (52). The Stanford University Administrative Panel on Laboratory Animal Care approved all animal protocols. Human fetal tissues were provided by Advanced Bioscience Resources (ABR; Alameda, CA) and were obtained in accordance with state and federal regulations.

VZV DNA PCR. Slides were deparaffinized, rehydrated in graded alcohols, and rinsed in sterile water. Tissue sections (5 sections, 5 μm each) were scraped with a sterile scalpel into a microcentrifuge tube containing 50 μl of DNA extraction buffer (10 mM Tris-Cl [pH 8.0], 1 mM EDTA, 1% Tween-20, 0.04% proteinase K). The DNA solution was incubated for 24 h at 42°C, after which the proteinase K was heat inactivated at 95°C for 10 min; the DNA extract was stored at −20°C until ready for analysis by PCR. In some cases, an additional purification round was performed using phenol-chloroform and DNA precipitation. PCR was performed using Elongase (Invitrogen) enzyme mix according to the manufacturer's instructions. PCR primers for the cellular β-globin gene (upper primer, 5′-GGTGGTCTACCCTTGGACCCAGAG-3′; lower primer, 5′-GTTCTCAGGATCCACGTGCAGCTT-3′) amplifies a 187-bp fragment, and PCR primers for VZV ORF9A (upper primer, 5′-ATGGGATCAATTACCGCTTCGT-3′; lower primer, 5′-CCACGTGCTGCGTAATACAGAA-3′) amplifies a 239-bp fragment. The PCR program was 35 cycles of 94°C for 1 min, 94°C for 30 s, 58°C for 30 s, 72°C for 30 s, and 72°C for 5 min.

VZV antibodies. Generation of a high-potency rabbit VZV IE63 antiserum was described in Zuranski et al. (53). Briefly, recombinant IE63 was obtained from cells infected with baculovirus expressing IE63 and purified using His-Bind resin (Novagen, Madison, WI) prior to rabbit immunization. The rabbit VZV IE63 antiserum and preimmune serum were further purified over a protein G column (Pierce, Rockford, IL) to obtain the IgG fraction and are referred to as anti-IE63-IgG and pre-IgG; purified IgG fractions were diluted 1:500 in PBS. The rabbit anti-GST-63-HIS (where GST is glutathione *S*-transferase) antiserum was kindly provided by S. Silverstein (Columbia University, New York, NY) and had been partially purified by negative adsorption over columns containing bacterial and mammalian cell proteins; this antibody was diluted 1:100 in phosphate-buffered saline (PBS) (27). Antibodies recognizing human neuronal synaptophysin (Zymed, Inc.) and VZV glycoprotein (g)E (Chemicon) were diluted as recommended by the manufacturer.

Antibody titration by ELISA. The sensitivity of detection of VZV IE63 protein by anti-IE63 antibodies was measured by whole VZV antigen enzyme-linked immunosorbent assay (ELISA). VZV positive-control sera (pooled human serum), pre-IgG, anti-IE63-IgG, and anti-GST-63-HIS were incubated for 2 h at room temperature in triplicate in wells coated with whole-cell extracts of VZV-infected (antigen) and uninfected (control) cells; 4-fold dilutions from 1:16 to 1:4,096 were tested. Detection was accomplished using a Vectastain ABC kit (Vector Laboratories) and orthophenyl diamine (OPD) peroxidase substrate. Color development was read with a SpectraMax 190 ELISA plate reader (Molecular Devices, Sunnyvale, CA). Values from triplicate wells were averaged, and control values were subtracted from antigen values.

Histochemical staining of melanins and lipofuscins. Nile blue A (Sigma) is certified by the Biological Stains Commission for staining of melanins and lipofuscins in histological sections. Differentiation of melanins and lipofuscins was performed using the method described by Lillie (25). Nile blue solution was prepared by gently boiling 0.5 g of Nile blue A in 100 ml of 1% sulfuric acid for 2 h. The solution was cooled, filtered, and made up to 100 ml before use. Tissue sections were deparaffinized, rehydrated in graded alcohols, and rinsed with distilled water in the typical manner. Slides were stained with 0.05% Nile blue in 1% sulfuric acid for 20 min, followed by quick clearing with 1% sulfuric acid. Nile blue ionogenically bonds with neuromelanin, which stains dark green. Cell nuclei and lipofuscins stain blue. Lipofuscin is extracted by dipping slides four times quickly in acetone, whereas melanin resists acetone extraction. Slides were mounted with glycerol-based medium.

Immunohistochemical staining. Deparaffinized and rehydrated tissue sections were immersed in citric acid-based antigen retrieval solution (Vector Laboratories), pH 6.0, and subjected to antigen retrieval using a standard protocol for formalin-fixed paraffin-embedded tissue sections. Immersed slides were microwaved using a 1.15-kW turntable microwave on full power for 5 min and then at 80% power for an additional 5 min. The slides were allowed to cool fully before staining. Cooled slides were incubated in 3.0% H_2O_2, washed with distilled water followed by PBS, and then incubated in blocking buffer for 10 min (IHC Select HRP Detection Kit; Millipore, Billerica, MA). Slides were then washed and incubated with pre-IgG or anti-IE63 antibodies for 1 h, followed by sequential incubations using an IHC Select HRP Detection Kit according to the manufacturer's instructions. The immunoperoxidase reaction product was visualized with 3,3-diaminobenzidine (DAB) solution (Vector Laboratories) supplemented with 0.1 M imidazole (pH 7.6). Tissue sections were counterstained with the blue nuclear counterstain hematoxylin or the biological stain Azure B (0.2%).

Immunohistochemical staining using the chromogen *p*-nitroblue tetrazolium choloride-5-bromo-4-chloro-3-indolyl phosphate (NBT-BCIP) was performed in a similar manner except that an IHC Select Alk-Phos Detection Kit (Millipore, Billerica, MA) was used for blocking, secondary antibody, and enzyme conjugation steps. The reaction product was visualized using the NBT-BCIP detection kit (Vector Laboratories).

TABLE 1. Clinical description of autopsy subjects

Specimen type, finding, and subject	Age (years)	Major diagnosis at death	No. of ganglia examined
Trigeminal ganglia			
Confirmed VZV positive			
K	72	Amyotrophic lateral sclerosis	1
T	63	Glioblastoma	2
U	80	Stroke	1
V	73	Bladder cancer	1
Undetermined VZV infection			
J	96	Alzheimer's disease	1
Dorsal root ganglia			
Confirmed VZV positive			
E	91	Alzheimer's disease	5
L	73	Prostate cancer	1
M	73	Dementia	2
N	48	Endocarditis sepsis	2
Q	93	Alzheimer's disease	1
R	84	Alzheimer's disease	1
W	67	Prostate cancer	3
X	73	Head injury	1
Y	73	Adenocarcinoma	1
Undetermined VZV infection			
G	82	Alzheimer's/Parkinson disease	1
H	68	Brain embolism/heart failure	1
S	37	Alzheimer's disease	1
P	93	Alzheimer's disease	1

Statistical analysis. Statistical analysis was performed using Excel, version 11.5.5.

RESULTS

Description of pathological specimens. Table 1 provides a description of 27 ganglion specimens obtained from the study population of 18 adults, with an age range of 37 to 96 years. These 6 TGG from five patients and 21 DRG from 13 patients were collected at autopsy and immediately fixed. All patients were without clinical evidence of herpes zoster when they died.

Detection of VZV DNA in cadaver ganglia. To test ganglion specimens for the presence of latent VZV DNA, DNA was extracted from tissue sections and subjected to PCR amplification using primers and probes for VZV ORF9A and the cellular β-globin gene. VZV ORF9A was amplified from TGG DNA from four subjects and from DRG DNA from nine subjects ($n = 13$). VZV DNA was not amplified in one TGG and four DRG ganglia after multiple attempts ($n = 5$). A representative gel is shown as Fig. 1. Based on the high seroprevalence rates for VZV IgG antibodies, it is likely that >95% of these adult subjects had a history of VZV infection and were therefore latently infected despite the negative PCR results in 5 of the 18 subjects. However, only those who were confirmed to have VZV DNA-positive ganglia were considered in the quantitative analysis presented in Table 2.

Comparison of antibody reagents for detection of IE63 by VZV ELISA and in neural cells in DRG xenografts infected with VZV in vivo. In preparation for staining tissue sections, the relative capacity of the anti-IE63-IgG and anti-GST-63-HIS antibodies to detect IE63 in a VZV-infected cell lysate was tested by whole VZV antigen ELISA. Anti-IE63-IgG was made using highly concentrated IE63 protein as the immunogen (53). The pre-IgG antibody, which is the paired serum obtained before rabbit immunization with purified IE63 protein, was evaluated in parallel. The anti-GST-63-HIS antibody was the reagent used to stain ganglion sections in the study by Lungu et al.; the paired preimmune serum for this antibody was not available (27). The highest dilution of anti-GST-63-HIS antibody that gave a signal above background in the VZV ELISA was 1:16 (Fig. 2). The highest positive dilution of anti-IE63-IgG antibody was 1:1,024, which represents a 64-fold increase in antigen recognition. These data demonstrate that the anti-IE63-IgG antibody is more sensitive than the anti-GST-63-HIS antibody for detection of IE63 protein in VZV-infected whole-cell lysates.

The IE63 antibody reagents and the preimmune control were also compared for their capacity to detect IE63 protein in human neural cells in DRG xenografts that were infected with VZV in SCID mice *in vivo*. Sections were examined from specimens obtained during the active infection phase (day 14) and the late phase (day 56) when viral proteins are no longer expressed; mock-infected DRG were also tested (52). Both anti-IE63 antibodies reacted with VZV proteins in the active infection specimens using the immunohistochemical staining protocol that employs the brown chromogen DAB and the blue nuclear counterstain hematoxylin. Antibody reactivity with IE63 protein was evident as brown deposits that often filled the entire neuronal cell nucleus and cytoplasm (Fig. 3B and C). No signal was observed when staining was performed with the pre-IgG reagent (Fig. 3A); no signal was observed in uninfected or persistently infected DRG xenografts (data not shown).

Immunohistochemical staining for IE63 in human cadaver ganglia using DAB/hematoxylin. When human cadaver ganglia sections were stained with anti-IE63-IgG and anti-GST-63-HIS antibodies using the DAB/hematoxylin protocol, the large brown deposits observed in neurons of VZV-infected DRG xenografts were seen only in rare sections from patient Q; IE63 protein was detected with both IE63 antibodies (Fig. 3H and I). Brown cytoplasmic deposits, consistent with lipofuscin, were

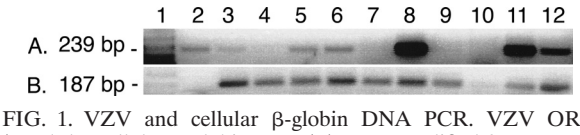

FIG. 1. VZV and cellular β-globin DNA PCR. VZV ORF9A (A) and the cellular β-globin gene (B) were amplified from extracted DNA. Lane 1, DNA ladder; lane 2, VZV genomic DNA; lanes 3 to 7, amplified DNA from subjects T (two blocks, left and right TGG), U, V, and P; lanes 8 and 9, VZV-infected SCID mouse skin xenografts (day 21 postinfection) and uninfected skin xenografts, respectively; lane 10, human fetal DNA; lanes 11 and 12, VZV-infected DRG xenografts at 14 days postinfection and latently infected DRG xenografts at 56 days postinfection, respectively.

TABLE 2. Percentage of pigment-containing neurons in 10 VZV DNA-positive ganglia from seven subjects

Sample no.	Pigment-containing cells in neurons as detected by:								
	Anti-pre-IgG			Anti-IE63-IgG			Anti-GST-63-HIS		
	No. of pigmented cells[a]	Total no. of neurons[b]	% Pigmented neurons	No. of pigmented cells[a]	Total no. of neurons	% Pigmented neurons	No. of pigmented cells[a]	Total no. of neurons[b]	% Pigmented neurons
E1	210	581	36.1	260	640	40.6	265	595	44.5
E2	222	565	39.3	203	440	46.1	305	630	48.4
K	64	90	71.1	49	85	57.6	70	100	70.0
L	192	780	24.6	180	680	26.4	210	770	27.2
M1	149	640	23.3	247	780	31.7	162	720	22.5
M2	210	545	38.5	195	610	32.0	269	500	53.8
N1	73	450	16.2	148	1,120	13.2	149	1,650	9.0
N2	92	760	12.1	48	650	7.4	111	610	18.2
Q	410	1,990	20.6	330	1,660	19.9	350	2,090	16.7
R	282	1,490	18.9	162	1,040	15.5	188	780	24.1

[a] Number of cells containing dark pigment deposits (lipofuscin, neuromelanin, or DAB).
[b] Total number of neurons counted per slide.

present in most sections (Fig. 3D, short arrows). For the most part, these golden-brown deposits appeared as unipolar or bipolar caps in large neurons, as described in previous investigations of VZV protein expression in ganglion sections (27, 29). We also observed darker granular deposits of various intensities (brown-black to black) in the cytoplasm of many neurons (Fig. 3D, large arrow). These deposits were primarily localized to the perinuclear region and were present regardless of the antibody solution that was applied, including the preimmune IgG (Fig. 3D and G).

Human cadaver ganglia contain neuromelanin, which confounds interpretation of immunohistochemical staining reactions using dark chromogens. The dark granular appearance of these deposits resembled the neuronal pigment neuromelanin. To verify the presence of neuromelanin in neurons in our human cadaver ganglion specimens, we stained the tissue sections with Nile blue solution, which renders neuromelanin granules green and lipofuscin granules blue (Fig. 4A and B).

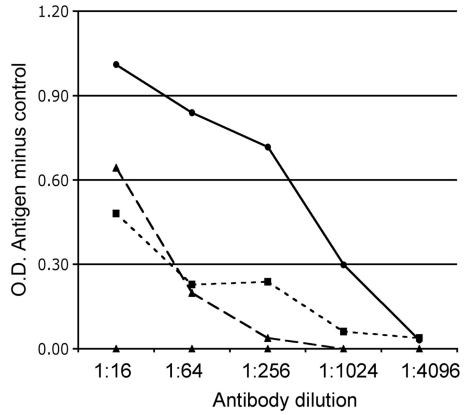

FIG. 2. Antibody titration by ELISA. Antibody sensitivity to VZV IE63 protein was measured by ELISA. Optical densitometry (OD) values for anti-pre-IgG (dotted line and filled square), anti-IE63-IgG (solid line and filled circle), and anti-GST-63-HIS (dashed line and filled triangle) sera are shown. Values from triplicate wells were averaged, and control values were subtracted from antigen values. Sera were serially diluted in 4-fold dilutions from 1:16 to 1:4,096. An OD of >0.3 is positive based on known positive and negative controls.

We also performed staining using the method described by Lillie for differentiation of melanins and lipofuscin (25). When sections from DRG and TGG were stained with Nile blue solution and then subjected to acetone extraction, only green deposits of melanin, which resist extraction, remained (Fig. 4C and D).

Since neuromelanin is a previously unidentified obstacle to assessment of VZV IE63 protein in neuronal ganglia, we performed a series of experiments to examine its potential to interfere with the interpretation of results using various staining methods. When ganglion sections were stained with antibody to synaptophysin, which is a neuron-specific protein, neither the brown chromogen DAB (data not shown) nor the black chromogen NBT-BCIP could be reliably differentiated from dark neuromelanin granules (Fig. 4E and F).

Quantification of neurons containing dark deposits after DAB/hematoxylin staining. Given evidence that differentiating dark neuronal pigment from dark chromogen deposits resulting from antigen-antibody interactions would be unreliable, we counted the number of ganglion cells that contained any dark deposits after DAB/hematoxylin staining with the pre-IgG or the IE63 antibody reagents, anti-IE63-IgG and anti-GST-63-HIS. As a further precaution, all slides examined were coded so that the reader did not know which antibody reagent had been applied to the slide. The number of cells containing dark deposits was determined by examining approximately 1,000 ganglion cells per section from seven patients who were confirmed to be VZV positive. The number of cells containing these dark deposits was compared in sequential sections, obtained from the same patient, that had been stained with pre-IgG or the IE63 antibody reagent anti-IE63-IgG or anti-GST-63-HIS. The results are summarized in Table 2.

On average, 30.1% of neurons in sections stained with pre-IgG contained cytoplasmic pigments. An equivalent percentage was detected in neurons stained with anti-IE63-IgG (29.1%) and anti-GST-63-HIS (33.5%). When the data were analyzed by a paired *t* test, no differences were detected in the frequencies of positive neurons in each subject in comparisons of pre-IgG and anti-IE63-IgG ($P = 0.32$) or anti-IE63-IgG and anti-GST-63-HIS ($P = 0.08$). The mean percent difference

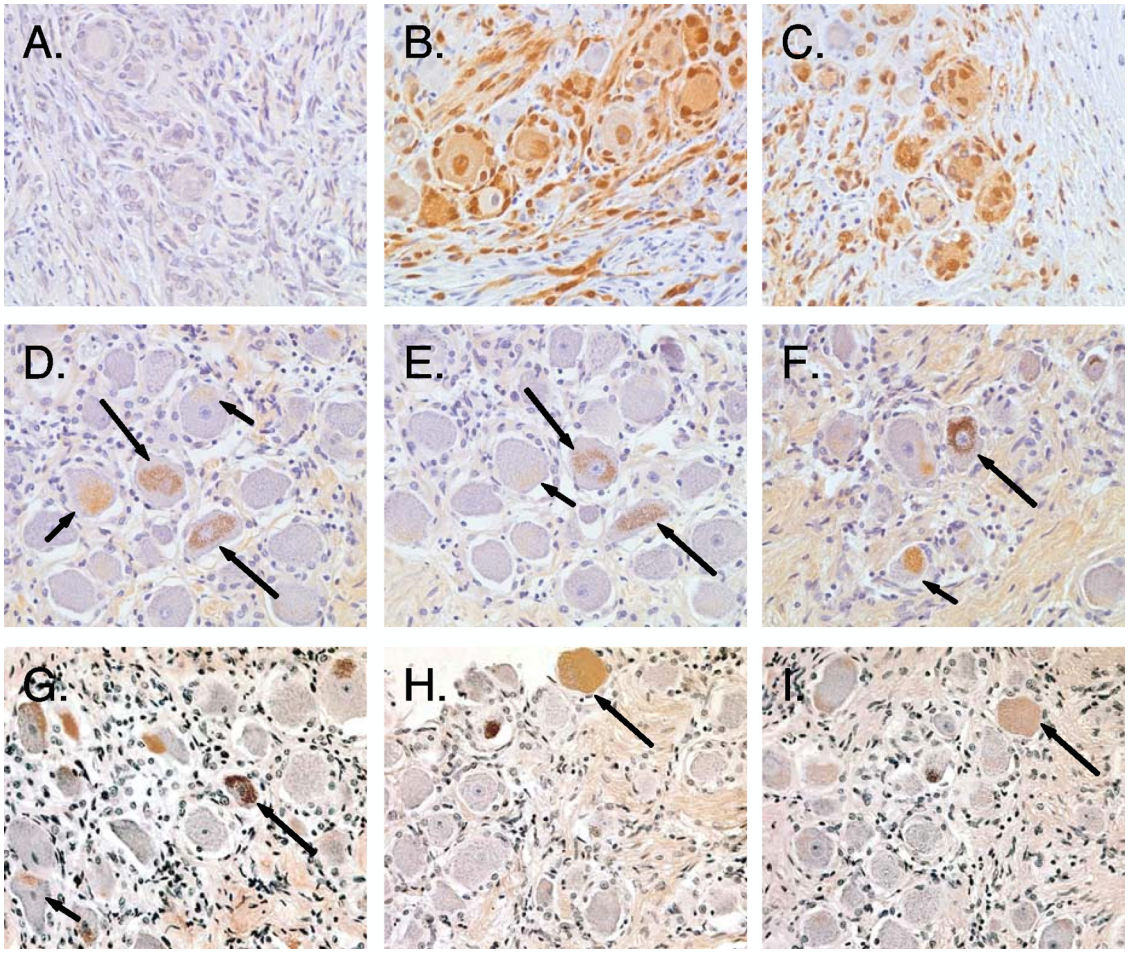

FIG. 3. IE63 immunohistochemical staining. (A to C) Representative panels from sections of VZV-infected DRG xenografts, 14 days postinfection stained with anti-pre-IgG antibody (A), anti-IE63-IgG antibody (B), and anti-GST-63-HIS antibody (C). (D to I) Representative panels from sections of human cadaver ganglia. DRG sections from patient E (D to F) and from patient Q (G to I) are shown. Sections are stained with anti-pre-IgG antibody (D and G), anti-IE63-IgG antibody (E and H), and anti-GST-63-HIS antibody (F and I). Short arrows in panels D to G indicate light-brown deposits consistent with lipofuscin while long arrows indicate darker deposits consistent with neuromelanin. Long arrows in panels H and I indicate neurons with staining of uncertain type (DAB or cellular pigment) in subject Q. Magnification, ×200.

between anti-pre-IgG- and anti-IE63-IgG-stained sections was −1.7%; the 95% confidence interval for the mean percent difference was −6.1% to 2.8%. Based on this approach using coded examination of sections and statistical analysis to address the nonspecific signal in ganglion neurons stained with dark chromogens, the data indicate that if IE63 protein is present in latently infected neurons, it is present in a very small proportion of neurons (no greater than 2.8%, with 95% confidence).

Immunohistochemical staining using the biological stain Azure B indicates that IE63 protein in human cadaver ganglia is rare. The biological stain Azure B is routinely used in diagnostic dermatopathology in the immunohistochemical staining of heavily pigmented tumors such as melanomas (17, 21, 31, 36). Like Nile blue, Azure B renders nuclei and lipofuscin blue and neuromelanin green, and it is compatible with visualization of DAB immunoreactivity (17, 21, 31, 36). We stained multiple ganglion sections from each of 18 patients (27 ganglia) using DAB chromogen and the biological stain Azure B to discriminate between IE63-immunoreactive cells and those containing neuromelanin and/or lipofuscin using high-potency anti-IE63-IgG or anti-pre-IgG. Five to 10 sections were examined per ganglion using anti-IE63-IgG; one section from each ganglion was stained in parallel with anti-pre-IgG. Sections from positive (VZV-infected) and negative (uninfected) control DRG xenografts were also stained with both antibodies. In total, we screened approximately 128,000 neurons in 169 sections from cadaver ganglia using this protocol. We detected DAB-positive IE63-immunoreactive cells in one ganglion from a single individual, subject Q.

Neurons in sections from subject Q did not exhibit any obvious cytopathology compared with neurons in sections from the other subjects that were IE63 negative; however, an inflammatory infiltrate was observed in the tissue section (Fig. 5A, white arrow). In two sections stained with anti-IE63-IgG, a small number of DAB-positive cells were observed (Fig. 5B, thin arrow). Azure B staining was sufficient to color neural pigment. Some staining was also observed within nerve fibers, but nonspecific staining of fibers sometimes occurred using the anti-pre-IgG antibody. At higher magnification (Fig. 5C, thin

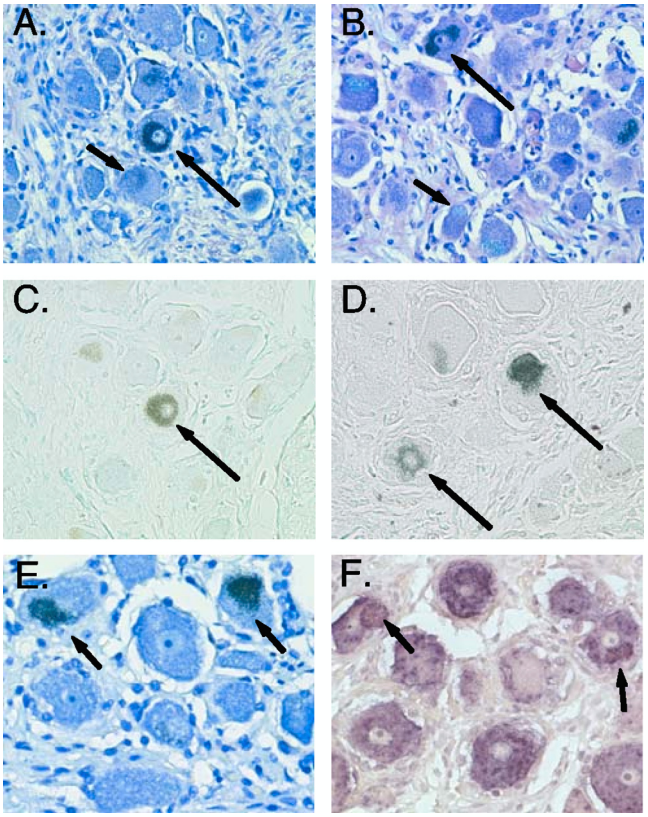

FIG. 4. Demonstration of neuromelanin. TGG sections from subject V (A and C) and DRG sections from subject M (B and D) are shown. Panels A and B are stained with Nile blue solution, which differentiates neuromelanin (long arrow and green staining) and lipofuscin (short arrow and blue staining). Panels C and D are stained with Nile blue solution after acetone extraction, which removes lipofuscin. Arrows show green-stained melanins which resist acetone extraction. Panels E and F are adjacent DRG sections from subject M that were stained with Azure B (E) or antibody to synaptophysin (NBT-BCIP; 4-min development). The short arrows in panels E and F indicate neuromelanin. Magnification for all images, ×200.

arrow), the IE63-specific signal was present in both the cytoplasm and neuronal cell nucleus. When the adjacent section was stained with a monoclonal antibody to the viral glycoprotein gE (Fig. 5D), a positive signal was detected in the cytoplasm of the same IE63-positive cell (Fig. 5B to D; compare the location of the nerve bundles in these sections, indicated by the thick black arrows, to the DAB-positive cell). Additional IE63-positive cells were present in the same section (Fig. 5E) and in the adjacent section. A mononuclear cell inflammatory infiltrate was observed in proximity to the IE63-positive cells (Fig. 5F, white arrow).

Staining with antisynaptophysin to demonstrate preservation of antigenicity. Seven of 27 cadaver ganglia that we examined were recently obtained at autopsy from the Stanford University Medical Center Department of Pathology; the others were archived paraffin blocks, which raised concerns of antigen preservation as a potential factor in the rare detection of IE63-positive neurons. To verify preservation of antigen, we stained sections from each of 27 ganglia with antibody to the neuronal cytoplasmic protein synaptophysin using the Azure B technique. Acceptable staining, in which >10% of neurons demonstrated synaptophysin expression and staining intensity was moderate to strong, was achieved in most cases. In three cases (patients K, R, and S), positive cells were clearly visible, but staining intensity was weak. Representative images are shown in Fig. 6. Synaptophysin is localized to neurosynaptic vesicles, which stain in a distinct cytoplasmic punctate pattern in DRG neurons (Fig. 6B) and TGG neurons (Fig. 6D). DAB immunoreactivity was readily visualized and could be distinguished from Azure B-stained neuronal pigment, even within the same cell (Fig. 6D, long arrow).

DISCUSSION

Defining the characteristics and mechanisms of latency remains a major challenge for understanding herpesvirus pathogenesis. Efforts to define the latency state have produced various observations and are particularly difficult for the human herpesviruses because of problems in obtaining relevant tissue specimens. In the case of VZV, reports about whether expression of VZV IE63 protein should be considered to be a characteristic of latently infected neurons have discrepancies. Mahalingam et al. and Kennedy et al. described IE63 protein expression as a rare event in a small proportion of cadaver ganglia from 16 and 20 subjects, respectively, whereas Lungu et al. and Grinfeld et al. reported abundant IE63 protein expression in ganglia from 3 and 10 patients (14, 19, 27, 29). Therefore, the aim of our investigation was to use some new approaches toward refining estimates of the numbers of neurons that express IE63 protein in human cadaver ganglia. Our analysis of 27 ganglia from 18 individuals supports the evidence that IE63 protein expression is unusual in ganglion neurons (19, 29).

In the first phase of our experiments, we found that the presence of neuronal cell pigments made signal interpretation difficult when sections from VZV-positive subjects were stained using a routine immunohistochemical protocol with the brown chromogen DAB. Whereas light-brown lipofuscin granules were mentioned as a possible source of interference in previous reports examining VZV protein expression, the darker neuromelanin granules were not. Neuromelanin is an age-related pigment that accumulates in autophagic vacuoles (referred to as granules) in the cytoplasm of catecholaminergic neurons, which are primarily found in the substantia nigra of the midbrain; however, these neurons also comprise a subpopulation in spinal ganglia of many species, including humans (6, 18, 23, 35, 48). Neuromelanin has been described in human TGG and DRG (3, 4, 10, 20, 22, 44). Neuronal pigments pose well-documented technical challenges to immunohistochemical staining in that the granules contain redox-active metals, primarily iron, which may participate in oxidation-reduction reactions which form the basis of immunohistochemical detection (1, 2, 12, 32, 33, 39, 46, 47). Whereas lipofuscin is primarily localized to unipolar or bipolar caps, neuromelanin is often observed throughout the cytoplasm (34, 39). Like lipofuscin, neuromelanin appears in human neurons after the first years of life, and so both are absent when fetal and neonatal tissues are used as negative controls (13, 34, 51). Our investigation of the sources of difficulty in interpreting IE63 staining confirmed

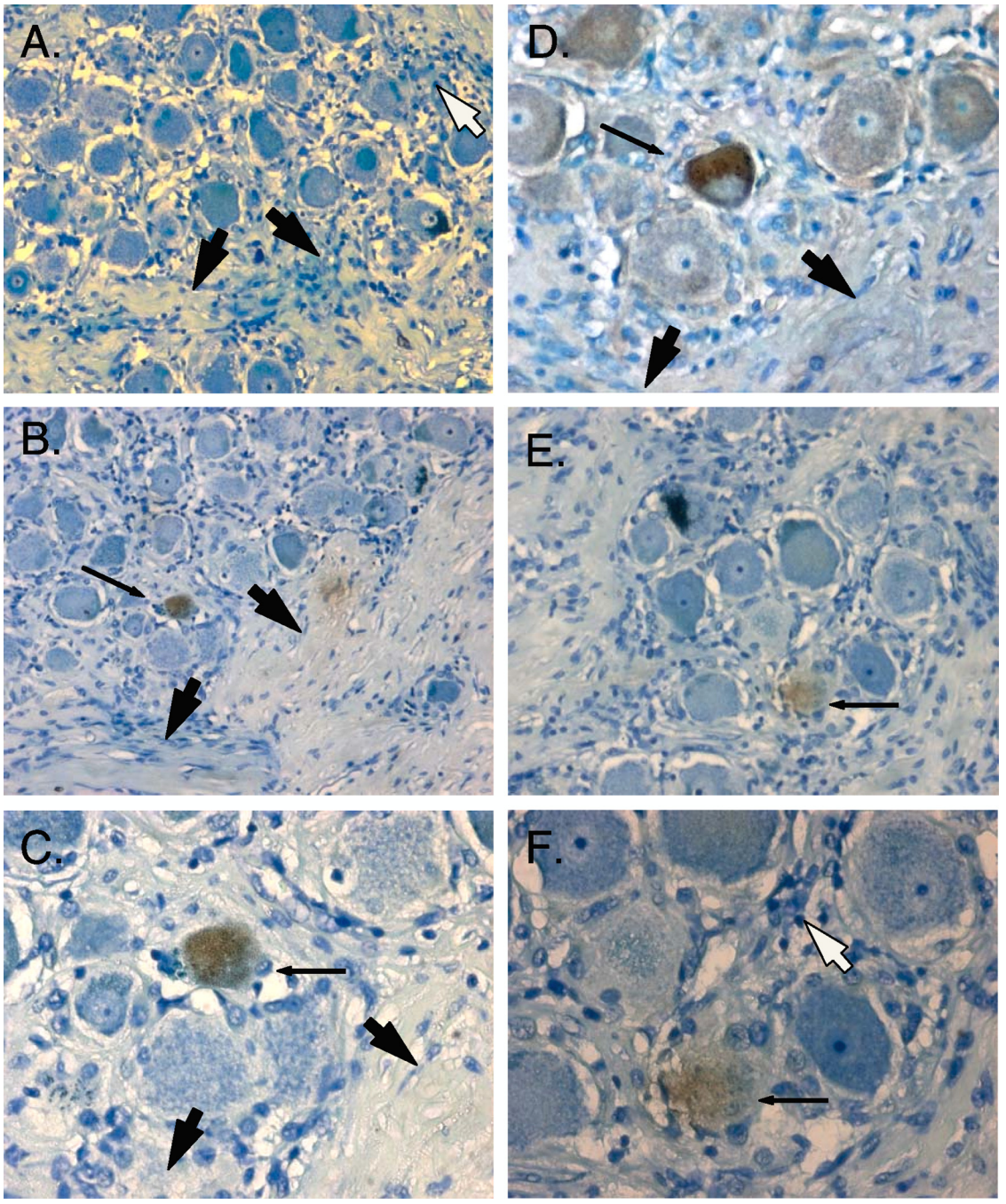

FIG. 5. IE63-positive staining in tissue sections from patient Q. Tissue sections from subject Q stained with anti-pre-IgG antibody (A), anti-IE63-IgG (B, C, E, and F), and anti-gE (D). Magnifications, ×100 (A, B, E) and ×200 (C, D, and F). Thin arrows in all sections indicate DAB-positive cells; thick black arrows indicate a fibrous band, as a reference point. White arrows in panels A and F indicate an inflammatory infiltrate.

that TGG and DRG neurons contain neuromelanin, which was shown using the Lillie method (25).

DAB and NBT-BCIP are considered to be the most sensitive chromogens for enzyme immunohistochemistry (11, 45). However, using dark-chromogen staining methods to stain neurons creates the challenge of differentiating dark deposits in neurons related to neural pigments from those representing true antigen-antibody interactions. As a strategy to reduce the subjective interpretation error, we used coded specimens and a statistical approach in which all pigment-containing neurons in ganglia from VZV-positive subjects were counted after staining with preimmune serum and two IE63 antibody reagents. The statistical analysis of these results indicated that IE63 protein, if present, is in a very small proportion ($\leq$2.8%) of neurons. As a second strategy, the biological stain Azure B was incorporated into the protocol in order to differentiate neuro-

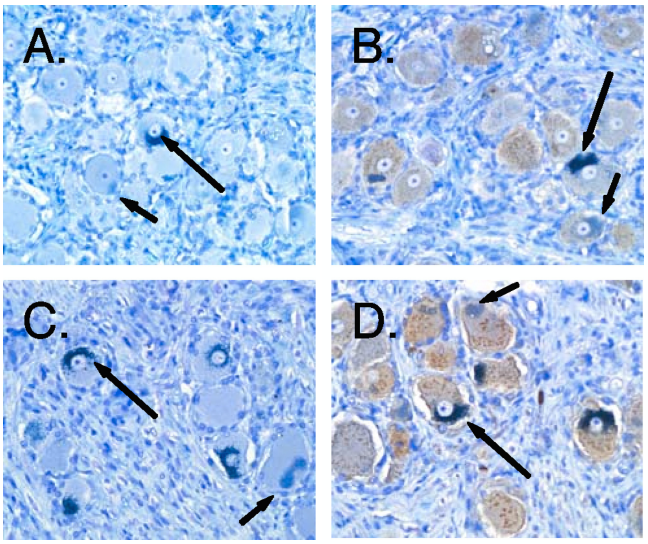

FIG. 6. Staining of autopsy ganglion sections with antibody synaptophysin. DRG sections from subject N and TGG sections from subject T were stained with antibody to synaptophysin (B and D) or negative-control solution (A and C) and poststained with Azure B solution. Neuromelanin deposits (long arrow) stain green, lipofuscin deposits (short arrow) stain blue. DAB immunoreactivity is apparent in most neurons and can easily be distinguished from neuronal pigment, even from within the same cell (D, long arrow). Magnification, ×200.

nal pigment from DAB deposition. Under these conditions, we detected IE63 protein in rare neurons (1 to 2 per section) in a few adjacent sections from one subject, but it was not detected in 26 ganglia from 17 individuals. We also observed coexpression of gE with IE63 in neurons proximate to an inflammatory infiltrate, suggesting a possible productive infection. To be sure that antigenicity was preserved, the ganglion sections were also stained for the neuron-specific protein synaptophysin, which has not been done in previous reports.

Our experience suggests that chromogen selection could contribute, in part, to the variation among reports about the frequency of IE63-positive neurons in cadaver ganglia. Using the dark chromogen NBT-BCIP to detect synaptophysin, a neuronal cell protein, we could not differentiate antigen-antibody staining from dark neuromelanin granules. Lungu et al. used this chromogen, whereas Mahalingam et al. used fresh fuschin chromogen, which produces an intense red color that may be more easily distinguished from dark-colored pigment granules (27, 29). The chromogen used to identify IE63-immunoreactive cells was not identified in the reports by Kennedy et al. and Grinfeld et al. (14, 19). We found that employing the Azure B modification made it possible to retain the high sensitivity of DAB while discriminating neural pigment from immunoreactivity.

Recently, Mueller et al. reported that IE63 exists in several modified forms, some of which may alter the affinity of certain anti-IE63 antibodies (30). However, our study employed two IE63 antibodies prepared using different approaches, one of which was used in a prior study that reported abundant IE63 expression in latently infected cadaver ganglia; therefore, differential posttranslational modification of IE63 is unlikely to explain the difference in results between our rare detection of IE63 protein and studies in which IE63 was more abundantly detected.

The chromogen development interval and use of antibodies derived from immunization with GST-fusion proteins are two other technical differences that may help to explain discrepancies in IE63 abundance, as reported by the four previous reports, and why our results reinforce the conclusions of the two that suggest only occasional IE63 expression. When we applied the long development step employed by Lungu et al. to ganglion sections stained with preimmune rabbit IgG, NBT-BCIP was deposited in pigment granules (data not shown). Antibodies derived from GST fusion constructs can exhibit cross-reactivity with endogenous GSTs; anti-GST reactivity may be especially problematic in aging neurons where mitochondrial GSTs are less efficiently degraded and where oxidatively modified GSTs may accumulate in response to certain neurological diseases associated with aging (5, 12, 37, 38, 40–42).

In addition to IE63, other VZV proteins have been detected by immunohistochemistry in latently infected neuronal ganglia, with various frequencies. Lungu et al. described IE62 and proteins encoded by ORFs 4, 21, and 29 in 9 to 24% of neurons in each of three ganglia examined from three patients (27). Grinfeld and Kennedy found IE62, ORF21, and ORF29 proteins in approximately 5 to 10% of neurons within some ganglia. Theil et al. employed the DAB chromogen and detected IE62 protein in ganglia from 8 of 21 individuals, with 2.5 to 7.3% of neurons IE62 positive; a subsequent report from the same group using DAB and 3-amino-9 ethyl carbazole (AEC) chromogens reported IE62 protein in all of 15 patients (32 of 37 DRG), with 6 to 39% IE62-positive neurons (15, 43). However, we suggest that the caveat about neuromelanin interference that we observed in staining for IE63 protein would apply to immunohistochemical detection of any viral or cellular proteins in neuronal ganglia.

In summary, developing a hypothesis about how VZV latency is maintained is complicated by the variation in the frequency and abundance of VZV protein expression described among investigations using cadaver ganglia. It is difficult to reconcile the high estimates of VZV protein expression in sensory ganglia using immunohistochemistry with estimates of VZV DNA burden using precise quantitative methods such as single-cell laser capture microdissection/PCR, which showed that a maximum of 6.9% of neurons harbored VZV genomes (49). Resolving these discrepancies is not straightforward because immunohistochemistry is the only available technique for testing human cadaver ganglia. Viral proteins can be detected by immunoblotting of lysates from productively infected tissues, but this approach is not likely to identify a protein expressed in a subpopulation of neurons among all ganglion cells. We reached our conclusion that the expression of VZV IE63 protein, which has been called a latency-associated protein, is uncommon and not a defining characteristic of VZV latency, based on the use of a staining method that reduces neuromelanin interference, a high-potency anti-IE63 antibody, and coded specimens. Our report becomes the third to indicate that the frequency of IE63-positive neurons is low. Moreover, our observations suggest that when IE63 protein is detected, its expression may indicate incipient reactivation from latency. Nevertheless, since no completely novel technique is available, no single study can resolve the discrepant reports about VZV

protein expression in latently infected neurons. Under these circumstances, more work must be done before a model of VZV latency and the state of the VZV genome during its persistence in the sensory neuron can be established. Such studies are important for developing better interventions against herpes zoster, which remains a common medical problem.

ACKNOWLEDGMENTS

This work was supported by grants from the National Institute of Allergy and Infectious Diseases (grant AI053846) and the National Cancer Institute (CA49605).

We thank Ruby Wong and the Division of Biostatistics at Stanford University Medical Center for assistance with statistical analysis.

REFERENCES

1. **Barden, H.** 1981. The biology and chemistry of neuromelanin, p. 155–180. *In* R. Sohal (ed.), Age pigments. Elsevier/North Holland Biomedical Press, Amsterdam, The Netherlands.
2. **Barden, H.** 1983. The presence of ethylenic bonds and vic-glycol groups in neuromelanin and lipofuscin in the human brain. J. Histochem. Cytochem. **31:**849–858.
3. **Beaver, D. L., H. L. Moses, and C. E. Ganote.** 1965. Electron microscopy of the trigeminal ganglion. 3. Trigeminal neuralgia. Arch. Pathol. **79:**571–582.
4. **Beaver, D. L., H. L. Moses, and C. E. Ganote.** 1965. Electron microscopy of the trigeminal ganglion. II. Autopsy study of human ganglia. Arch. Pathol. **79:**557–570.
5. **Beiswanger, C. M., M. H. Diegmann, R. F. Novak, M. A. Philbert, T. L. Graessle, K. R. Reuhl, and H. E. Lowndes.** 1995. Developmental changes in the cellular distribution of glutathione and glutathione S-transferases in the murine nervous system. Neurotoxicology **16:**425–440.
6. **Brumovsky, P., M. J. Villar, and T. Hokfelt.** 2006. Tyrosine hydroxylase is expressed in a subpopulation of small dorsal root ganglion neurons in the adult mouse. Exp. Neurol. **200:**153–165.
7. **Cohen, J. I., S. E. Straus, and A. Arvin.** 2007. Varicella-zoster virus replication, pathogenesis and management, p. 2773–2818. *In* D. M. Knipe, P. M. Howley, D. E. Griffin, R. A. Lamb, M. A. Martin, B. Roizman, and S. E. Straus (ed.), Fields virology, 5th ed. Lippincott Williams & Wilkins, Philadelphia, PA.
8. **Cohrs, R., R. Mahalingam, A. N. Dueland, W. Wolf, M. Wellish, and D. H. Gilden.** 1992. Restricted transcription of varicella-zoster virus in latently infected human trigeminal and thoracic ganglia. J. Infect. Dis. **166**(Suppl. 1)**:**S24—S29.
9. **Croen, K. D., J. M. Ostrove, L. J. Dragovic, and S. E. Straus.** 1988. Patterns of gene expression and sites of latency in human nerve ganglia are different for varicella-zoster and herpes simplex viruses. Proc. Natl. Acad. Sci. U. S. A. **85:**9773–9777.
10. **DeCastro, F.** 1932. Sensory ganglia of the cranial and spinal nerves: normal and pathological. *In* W. Penfield (ed.), Cytology and cellular pathology of the nervous system. Paul B. Hoeber, Inc., New York, NY.
11. **De Jong, A. S., M. Van Kessel-van Vark, and A. K. Raap.** 1985. Sensitivity of various visualization methods for peroxidase and alkaline phosphatase activity in immunoenzyme histochemistry. Histochem. J. **17:**1119–1130.
12. **Double, K. L., V. N. Dedov, H. Fedorow, E. Kettle, G. M. Halliday, B. Garner, and U. T. Brunk.** 2008. The comparative biology of neuromelanin and lipofuscin in the human brain. Cell Mol. Life Sci. **65:**1669–1682.
13. **Goyal, V. K.** 1982. Lipofuscin pigment accumulation in human brain during aging. Exp. Gerontol. **17:**481–487.
14. **Grinfeld, E., and P. G. Kennedy.** 2004. Translation of varicella-zoster virus genes during human ganglionic latency. Virus Genes **29:**317–319.
15. **Hufner, K., T. Derfuss, S. Herberger, K. Sunami, S. Russell, I. Sinicina, V. Arbusow, M. Strupp, T. Brandt, and D. Theil.** 2006. Latency of alpha-herpes viruses is accompanied by a chronic inflammation in human trigeminal ganglia but not in dorsal root ganglia. J. Neuropathol. Exp. Neurol. **65:**1022–1030.
16. **Hynd, M. R., J. M. Lewohl, H. L. Scott, and P. R. Dodd.** 2003. Biochemical and molecular studies using human autopsy brain tissue. J. Neurochem. **85:**543–562.
17. **Kamino, H., and S. T. Tam.** 1991. Immunoperoxidase technique modified by counterstain with azure B as a diagnostic aid in evaluating heavily pigmented melanocytic neoplasms. J. Cutan. Pathol. **18:**436–439.
18. **Katz, D. M., K. A. Markey, M. Goldstein, and I. B. Black.** 1983. Expression of catecholaminergic characteristics by primary sensory neurons in the normal adult rat in vivo. Proc. Natl. Acad. Sci. U. S. A. **80:**3526–3530.
19. **Kennedy, P. G., E. Grinfeld, and J. E. Bell.** 2000. Varicella-zoster virus gene expression in latently infected and explanted human ganglia. J. Virol. **74:** 11893–11898.
20. **Kishikawa, M., M. Matsumoto, M. Iseki, H. Kondo, O. Shimada, N. Tsuda, and H. Fujii.** 1988. Quantitative study of neurons with intracytoplasmic pigments in dorsal root ganglia: atomic bomb and aging. Acta Med. Nagasaki **33:**58–62.
21. **Kligora, C. J., K. P. Fair, M. S. Clem, and J. W. Patterson.** 1999. A comparison of melanin bleaching and azure blue counterstaining in the immunohistochemical diagnosis of malignant melanoma. Mod. Pathol. **12:**1143–1147.
22. **Koistinaho, J., K. Hartikainen, K. Hatanpaa, and A. Hervonen.** 1989. Age pigments in different populations of peripheral neurons in vivo and in vitro. Adv. Exp. Med. Biol. **266:**49–59.
23. **Kummer, W., I. L. Gibbins, P. Stefan, and V. Kapoor.** 1990. Catecholamines and catecholamine-synthesizing enzymes in guinea-pig sensory ganglia. Cell Tissue Res. **261:**595–606.
24. **Levin, M. J., G. Y. Cai, M. D. Manchak, and L. I. Pizer.** 2003. Varicella-zoster virus DNA in cells isolated from human trigeminal ganglia. J. Virol. **77:**6979–6987.
25. **Lillie, R. D.** 1956. A Nile blue staining technic for the differentiation of melanin and lipofuscins. Stain Technol. **31:**151–153.
26. **Lungu, O., P. W. Annunziato, A. Gershon, S. M. Staugaitis, D. Josefson, P. LaRussa, and S. J. Silverstein.** 1995. Reactivated and latent varicella-zoster virus in human dorsal root ganglia. Proc. Natl. Acad. Sci. U. S. A. **92:**10980–10984.
27. **Lungu, O., C. A. Panagiotidis, P. W. Annunziato, A. A. Gershon, and S. J. Silverstein.** 1998. Aberrant intracellular localization of Varicella-Zoster virus regulatory proteins during latency. Proc. Natl. Acad. Sci. U. S. A. **95:** 7080–7085.
28. **Lynch, J. M., T. K. Kenyon, C. Grose, J. Hay, and W. T. Ruyechan.** 2002. Physical and functional interaction between the varicella zoster virus IE63 and IE62 proteins. Virology **302:**71–82.
29. **Mahalingam, R., M. Wellish, R. Cohrs, S. Debrus, J. Piette, B. Rentier, and D. H. Gilden.** 1996. Expression of protein encoded by varicella-zoster virus open reading frame 63 in latently infected human ganglionic neurons. Proc. Natl. Acad. Sci. U. S. A. **93:**2122–2124.
30. **Mueller, N. H., L. L. Graf, D. Orlicky, D. Gilden, and R. J. Cohrs.** 2009. Phosphorylation of the nuclear form of varicella-zoster virus immediate-early protein 63 by casein kinase II at serine 186. J. Virol. **83:**12094–12100.
31. **Nadji, M.** 1986. Immunoperoxidase techniques. I. Facts and artifacts. Am. J. Dermatopathol. **8:**32–36.
32. **Novikoff, A. B., W. Y. Shin, and J. Drucker.** 1961. Mitochondrial localization of oxidative enzymes: staining results with two tetrazolium salts. J. Biophys. Biochem. Cytol. **9:**47–61.
33. **Pearse, A.** 1985. Pigment and pigment precursors, p. 874–928. *In* A. Pearse (ed.), Histochemistry, theoretical and applied, 4th ed., vol. 2. Churchill Livingstone, London, United Kingdom.
34. **Porta, E. A.** 2002. Pigments in aging: an overview. Ann. N. Y. Acad. Sci. **959:**57–65.
35. **Price, J., and A. W. Mudge.** 1983. A subpopulation of rat dorsal root ganglion neurones is catecholaminergic. Nature **301:**241–243.
36. **Ramos-Vara, J. A.** 2005. Technical aspects of immunohistochemistry. Vet. Pathol. **42:**405–426.
37. **Ryle, C. M., and T. J. Mantle.** 1984. Studies on the glutathione S-transferase activity associated with rat liver mitochondria. Biochem. J. **222:**553–556.
38. **Sultana, R., and D. A. Butterfield.** 2004. Oxidatively modified GST and MRP1 in Alzheimer's disease brain: implications for accumulation of reactive lipid peroxidation products. Neurochem. Res. **29:**2215–2220.
39. **Sulzer, D., E. Mosharov, Z. Talloczy, F. A. Zucca, J. D. Simon, and L. Zecca.** 2008. Neuronal pigmented autophagic vacuoles: lipofuscin, neuromelanin, and ceroid as macroautophagic responses during aging and disease. J. Neurochem. **106:**24–36.
40. **Terman, A., and U. T. Brunk.** 2004. Lipofuscin. Int. J. Biochem. Cell Biol. **36:**1400–1404.
41. **Terman, A., and U. T. Brunk.** 2006. Oxidative stress, accumulation of biological "garbage," and aging. Antioxid. Redox. Signal. **8:**197–204.
42. **Terman, A., B. Gustafsson, and U. T. Brunk.** 2007. Autophagy, organelles and ageing. J. Pathol. **211:**134–143.
43. **Theil, D., I. Paripovic, T. Derfuss, S. Herberger, M. Strupp, V. Arbusow, and T. Brandt.** 2003. Dually infected (HSV-1/VZV) single neurons in human trigeminal ganglia. Ann. Neurol. **54:**678–682.
44. **Thomas, P., F. Scaravilli, and A. Belai.** 1993. Pathologics alterations in cell bodies of peripheral neurons in neuropathy, p. 476–513. *In* P. Dyck, P. Thomas, and J. Griffin (ed.), Peripheral neuropathy, 3rd ed., vol. 1. W. B. Saunders Co., Philadelphia, PA.
45. **Trojanowski, J. Q., M. A. Obrocka, and V. M. Lee.** 1983. A comparison of eight different chromogen protocols for the demonstration of immunoreactive neurofilaments or glial filaments in rat cerebellum using the peroxidase-antiperoxidase method and monoclonal antibodies. J. Histochem. Cytochem. **31:**1217–1223.
46. **Valembois, P., and M. Lassegues.** 1995. In vitro generation of reactive oxygen species by free coelomic cells of the annelid Eisenia fetida andrei: an analysis by chemiluminescence and nitro blue tetrazolium reduction. Dev. Comp. Immunol. **19:**195–204.
47. **Valembois, P., J. Seymour, and M. Lassegues.** 1994. Evidence of lipofuscin and melanin in the brown body of the earthworm Eisenia fetida andrei. Cell Tissue Res. **277:**183–188.

48. **Vega, J. A., F. Amenta, L. C. Hernandez, and M. E. del Valle.** 1991. Presence of catecholamine-related enzymes in a subpopulation of primary sensory neurons in dorsal root ganglia of the rat. Cell Mol. Biol. **37:**519–530.
49. **Wang, K., T. Y. Lau, M. Morales, E. K. Mont, and S. E. Straus.** 2005. Laser-capture microdissection: refining estimates of the quantity and distribution of latent herpes simplex virus 1 and varicella-zoster virus DNA in human trigeminal ganglia at the single-cell level. J. Virol. **79:**14079–14087.
50. **Waxman, S. G.** 2003. Clinical neuroanatomy. Lange Medical Books/McGraw-Hill, New York, NY.
51. **Zecca, L., F. A. Zucca, H. Wilms, and D. Sulzer.** 2003. Neuromelanin of the substantia nigra: a neuronal black hole with protective and toxic characteristics. Trends Neurosci. **26:**578–580.
52. **Zerboni, L., C. C. Ku, C. D. Jones, J. L. Zehnder, and A. M. Arvin.** 2005. Varicella-zoster virus infection of human dorsal root ganglia in vivo. Proc. Natl. Acad. Sci. U. S. A. **102:**6490–6495.
53. **Zuranski, T., H. Nawar, D. Czechowski, J. M. Lynch, A. Arvin, J. Hay, and W. T. Ruyechan.** 2005. Cell-type-dependent activation of the cellular EF-1α promoter by the varicella-zoster virus IE63 protein. Virology **338:**35–42.